

# Fundamental constants and tests of theory in Rydberg states of hydrogenlike ions<sup>1</sup>

Ulrich D. Jentschura, Peter J. Mohr, Joseph N. Tan, and Benedikt J. Wundt

**Abstract:** A comparison of precision frequency measurements to quantum electrodynamic (QED) theoretical predictions can be used to test theory and to obtain information regarding fundamental constants. We find that for Rydberg states, theoretical uncertainties due to the problematic nuclear size correction are very small. With the help of QED calculations, the largest remaining source of uncertainty can be eliminated. Theoretical predictions, taking advantage of the latest theoretical results, in combination with planned experiments, can lead to an improved value for the Rydberg constant.

PACS Nos: 06.20.Jr, 12.20.Ds, 31.30.jf

**Résumé :** Une comparaison des mesures de fréquence de précision avec les prédictions théoriques de l'électrodynamique quantique (QED), peut être utilisée pour tester la théorie et obtenir de l'information sur les constantes fondamentales.

Nous trouvons que pour les états de Rydberg, les incertitudes théoriques dues aux corrections problématiques venant de la grosseur finie du noyau restent faibles. Avec l'aide des calculs QED, la plus importante source restante d'incertitudes peut être éliminée. Les prédictions théoriques qui prennent avantage des résultats théoriques les plus récents, en combinaison avec des expériences planifiées, peuvent mener à des valeurs améliorées pour la constante de Rydberg.

[Traduit par la Rédaction]

## 1. Introduction

Quantum electrodynamics (QED) makes very precise predictions of various physical quantities, most of which can be measured very accurately using high-precision spectroscopy. As is well-known, this makes QED one of the best tested and the most precise theories developed so far. Some of the most accurately known fundamental constants are, in fact, determined from a combination of QED theory and experiment.

In this work, we focus on hydrogenlike atomic systems. With the availability of optical frequency combs [1], the transition frequency for the 1S–2S transition in hydrogen can be measured with a relative uncertainty of  $1.4 \times 10^{-14}$  [2]. However, the theoretical predictions for these levels suffer from uncertainties due to nuclear effects. Indeed, in the 2006 CODATA adjustment of the fundamental constants [3], the proton radius is determined mainly from hydrogen and deuterium spectroscopy. There are plans for independent measurements of the nuclear radius of the lightest nuclei,

but so far these have not met with success. In fact, one might ask why the Rydberg constant, which is the most accurately known fundamental constant, can be determined only to a relative uncertainty of  $6.6 \times 10^{-12}$ , which is very crude in comparison to the most accurate measurement ( $1.4 \times 10^{-14}$ ). The reason lies with the nuclear size effect, and a possibility for overcoming this restriction is with the use of Rydberg states in hydrogenlike ions with a medium nuclear charge number.

In Rydberg states, the electron is highly excited, and from a classical point of view, “far away” from the nucleus: the nuclear size correction becomes negligible. Further, the coefficients multiplying the higher-order QED corrections are much smaller than for states with lower angular momenta, enhancing the theoretical accuracy that can be reached with QED corrections up to a specific order. The largest remaining uncertainty, due to higher-order binding corrections to the one-photon self-energy shift, can be removed with the aid of new calculations [4]. Some of the new theoretical predictions for the fine-structure transition frequencies among Rydberg states have a relative uncertainty as small as  $10^{-16}$  (neglecting additional uncertainty from the Rydberg constant and from the electron–nucleus mass ratio). Therefore, a high precision measurement of various transition frequencies of Rydberg states combined with the theoretical calculations we will present here, could yield a new, more precise value for the Rydberg constant.

In past work by other groups [5], circular Rydberg states of hydrogen in an 80 K atomic beam have been analyzed.<sup>3</sup> A precision measurement of transition wavelengths in the millimetre region provided a determination of the Rydberg constant with a relative uncertainty of  $2.1 \times 10^{-11}$  [5]<sup>3</sup>. This is not enough to reduce the uncertainty of the Rydberg constant with respect to the CODATA value, but it shows that precision measurements on Rydberg states are possible.

Received 16 October 2008. Accepted 27 October 2008.  
Published on the NRC Research Press Web site at [cjp.nrc.ca](http://cjp.nrc.ca) on 5 September 2009.

**U.D. Jentschura.**<sup>2</sup> Department of Physics, Missouri University of Science and Technology, Rolla MO 65409-0640, USA.

**P.J. Mohr and J.N. Tan.** National Institute of Standards and Technology, Mail Stop 8420, Gaithersburg, MD 20899-8420, USA.

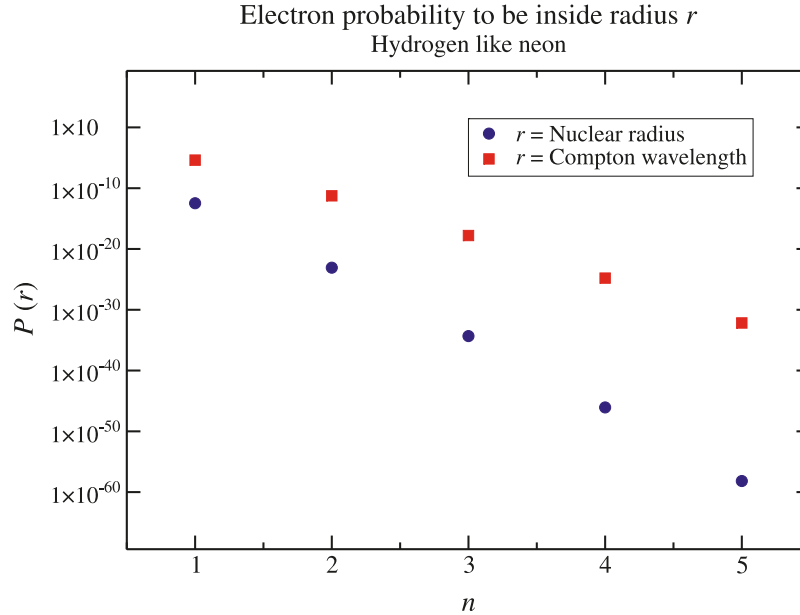
**B.J. Wundt.** Max-Planck-Institut für Kernphysik, Postfach 10 39 80, 69029 Heidelberg, Germany.

<sup>1</sup>This paper was presented at the International Conference on Precision Physics of Simple Atomic Systems, held at University of Windsor, Windsor, Ontario, Canada on 21–26 July 2008.

<sup>2</sup>Corresponding author (e-mail: [ulj@mst.edu](mailto:ulj@mst.edu)).

<sup>3</sup>D. Kleppner. Private communication. 2001.

**Fig. 1.** Graph showing the electron probability to be inside radius  $r$  in hydrogenlike neon in the state with  $l = n - 1$ .



Using a femtosecond laser, it may also be possible to use optical frequency combs to measure optical transitions between Rydberg states with at least the same precision as for lower lying states.

## 2. Theory

In this section we describe the theory of all the necessary corrections for Rydberg states. We also show how the known theoretical expressions simplify for Rydberg states and further give results of our calculation, which eliminates the largest remaining source of uncertainty.

To accurately predict the energy levels of atoms and ions it is vital to recall that the nucleus is not pointlike but occupies a finite region of space. For states with high orbital angular momenta  $l$ , the probability for the electron to be found within a short distance  $r$  of the nucleus is very low. For a Rydberg state of a hydrogenlike ion with charge number  $Z$ , high principal quantum number  $n$ , and angular momentum  $l = n - 1$ , this probability is,

$$P(r) = \int_{|x|<r} d\mathbf{x} |\psi(\mathbf{x})|^2 \approx \frac{1}{(2n+1)!} \left( \frac{2Zr}{na_0} \right)^{2n+1} \quad (1)$$

where  $a_0$  is the Bohr radius. Because of this strong damping, effects arising from interactions near or within the nucleus are negligible. If we take  $r$  to be the nuclear radius, then the high power  $(r/a_0)^{2n+1}$  together with the factorial in the denominator, leads to an almost complete suppression of nuclear effects for circular or near-circular Rydberg states. An example of the probability  $P(r)$  as a function of  $n$  for hydrogenlike neon, is shown in Fig. 1.

As discussed in [3], theoretical predictions for energy levels include many effects that cause deviations from Dirac theory. For Rydberg states, corrections due to effects of the nucleus are negligible. Thus, a Rydberg-state energy level  $E_n$  may be written as a sum of the Dirac energy  $E_{\text{DM}}$  (with nuclear motion corrections included), the relativistic recoil correction  $E_{\text{RR}}$ , and radiative corrections  $E_{\text{QED}}$ :  $E_n = E_{\text{DM}} +$

$E_{\text{RR}} + E_{\text{QED}}$ , for  $l \geq 2$ . The difference between the Dirac eigenvalue and the rest mass of the electron is proportional to,

$$\begin{aligned} \alpha^2 m_e c^2 D &= E_D - m_e c^2 \\ &= m_e c^2 \left( \left[ 1 + \frac{(Z\alpha)^2}{(n-\delta)^2} \right]^{-1/2} - 1 \right) \end{aligned} \quad (2)$$

where  $\delta = |\kappa| - \sqrt{\kappa^2 - (Z\alpha)^2}$ ,  $\kappa = (-1)^{l+j+1/2}(j+1/2)$  is the Dirac spin-angular quantum number,  $j$  is the total angular momentum quantum number, and  $\alpha$  is the fine-structure constant.  $D$  can be expanded to give the known Schrödinger energy and the fine-structure terms,

$$\alpha^2 D = -\frac{(Z\alpha)^2}{2n^2} + \left( \frac{3}{8n} - \frac{1}{2j+1} \right) \frac{(Z\alpha)^4}{n^3} + \dots \quad (3)$$

The Dirac energy level, taking into account the leading nuclear motion effects but not including the electron or nucleus rest energy, is given by [6],

$$E_{\text{DM}} = 2hcR_\infty \left[ \mu_r D - \frac{r_N \mu_r^3 \alpha^2}{2} D^2 + \frac{r_N^2 \mu_r^3 Z^4 \alpha^2}{2n^3 \kappa (2l+1)} \right] \quad (4)$$

where  $h$  is the Planck constant,  $c$  is the speed of light,  $R_\infty = \alpha^2 m_e c / 2h$  is the Rydberg constant,  $r_N = m_e / m_N$  is the ratio of the electron to the nucleus mass, and  $\mu_r = 1/(1+r_N)$  is the ratio of the reduced mass to the electron mass.

The other two terms are relativistic corrections to the Dirac energy. The relativistic recoil corrections account for the effect of the nuclear motion, and the radiative corrections are those of the electron. First, we consider the relativistic recoil. Its leading order (lo) term was given for a general state by Erickson [7]. For a Rydberg state with  $l \geq 2$  it is given as,

$$E_{\text{RR},\text{lo}} = 2hcR_\infty \frac{r_N Z^5 \alpha^3}{\pi n^3} \mu_r^3 \left[ -\frac{8}{3} \ln k_0(n, l) - \frac{7}{3} a_n \right] \quad (5)$$

where  $\ln k_0(n, l)$  is the Bethe logarithm and

$$a_n = \frac{1}{l(l+1)(2l+1)} \quad (6)$$

for  $l \geq 2$ . An instructive review of the derivation of this expression can be found in [8]. To leading order in the mass ratio, a semi-analytic expansion in  $Z\alpha$  leads to higher-order (ho) corrections,

$$E_{RR,ho} = 2hcR_\infty \frac{Z^6 \alpha^4 r_N}{n^3} [D_{60} + D_{72} \ln^2(Z\alpha)^{-2} + \dots] \quad (7)$$

where the first index of the coefficients denotes the power of  $(Z\alpha)$  and the second the power of the logarithm of

$(Z\alpha)^{-2}$ . (This indexing is common notation in QED and will be used throughout this paper.) The  $D_{60}$  coefficient has been determined in [9–13]. For  $l \geq 2$  it is,

$$D_{60} = \left[ 3 - \frac{l(l+1)}{n^2} \right] \frac{2}{(4l^2 - 1)(2l+3)} \quad (8)$$

The  $D_{72}$  coefficient was recently calculated in [14, 15] and is found to be zero for states with  $l > 0$ . The complete relativistic recoil correction for circular or near-circular Rydberg states is then given as,

$$\begin{aligned} E_{RR} &= E_{RR,ho} + E_{RR,lo} \\ &= 2hcR_\infty \frac{r_N Z^5 \alpha^3}{\pi n^3} \left\{ \mu_r^3 \times \left[ -\frac{8}{3} \ln k_0(n, l) - \frac{7}{3l(l+1)(2l+1)} \right] + \pi Z\alpha \left[ 3 - \frac{l(l+1)}{n^2} \right] \frac{2}{(4l^2 - 1)(2l+3)} + \dots \right\} \end{aligned} \quad (9)$$

Besides  $D_{72}$ , no further terms are known, which means we have to estimate the uncertainty introduced by cutting the expansion after the known terms. Since there might be a contribution from a  $D_{71}$  term, we adopt the procedure of estimating the uncertainty as being  $(Z\alpha)\ln(Z\alpha)^{-2}$  times the contribution of the last term on the right-hand side of (9).

Next, we will consider the corrections introduced by QED. Here again, the features of Rydberg states allow simplifications to be made. Similarly, as for the relativistic recoil, the self-energy corrections can be expanded into a semi-analytic series in  $(Z\alpha)$  that yields for Rydberg states,

$$E_{QED} = 2hcR_\infty \frac{Z^4 \alpha^3}{\pi n^3} \left\{ A_{40} + A_{61}(Z\alpha)^2 \ln(Z\alpha)^{-2} + (Z\alpha)^2 G(Z\alpha) + \frac{\alpha}{\pi} [B_{40} + \dots] + \left(\frac{\alpha}{\pi}\right)^2 [C_{40} + \dots] \right\} \quad (10)$$

The  $A$  coefficients arise from the one-photon QED corrections, while those starting with  $B$  and  $C$  come from the two-photon and three-photon QED corrections, respectively. Furthermore, the non-vanishing contributions of  $B_{40}$  and  $C_{40}$  can be combined with  $A_{40}$  to give the correction due to the electron magnetic anomaly  $a_e$ , in leading order. This leads to the compact result,

$$\begin{aligned} E_{QED} &= 2hcR_\infty \frac{Z^4 \alpha^2}{n^3} \left\{ -\mu_r^2 \frac{a_e}{\kappa(2l+1)} + \mu_r^3 \frac{\alpha}{\pi} \left[ -\frac{4}{3} \ln k_0(n, l) + \frac{32 \cdot 3n^2 - l(l+1)}{3n^2} \right. \right. \\ &\quad \left. \left. + \frac{(2l-2)!}{(2l+3)!} (Z\alpha)^2 \ln \left( \frac{1}{\mu_r(Z\alpha)^2} \right) + (Z\alpha)^2 G(Z\alpha) \right] \right\} \end{aligned} \quad (11)$$

for the self-energy corrections to Rydberg states. In the determination of the electron magnetic moment anomaly, terms with a high number of loops have to be considered. Since the experimental value for  $a_e$  has been measured very precisely [16], it is possible to use the experimental value of

$$a_e = 1.159\,652\,180\,73(28) \times 10^{-3} \quad (12)$$

obtained with a one-electron cyclotron [16]. Even though this term is known theoretically up to three-loop order, using the experimental value eliminates uncertainties introduced through uncalculated higher-order terms.

To reach the precision necessary to set a more precise value for the Rydberg constant, it is essential to evaluate the self-energy remainder functions  $G(Z\alpha)$  as well. The leading terms of  $G(Z\alpha)$  are expected to be of the form,

$$G(Z\alpha) = A_{60} + A_{81}(Z\alpha)^2 \ln(Z\alpha)^{-2} + A_{80}(Z\alpha)^2 + \dots + \frac{\alpha}{\pi} B_{60} + \dots + \left(\frac{\alpha}{\pi}\right)^2 C_{60} + \dots \quad (13)$$

The  $A_{60}$  coefficient would be the major source of theoretical uncertainty for Rydberg states. Both contributions from order  $\alpha(Z\alpha)^8$  are so far unknown but are expected to be small. Only the vacuum polarization contribution to  $A_{80}$  is known [17] and is extremely small. The two-photon diagrams lead to additional contributions. The  $B_{60}$  coefficient is the only one of those that is nonzero for states with  $l \geq 2$  [3, 18]. So far, it has been calculated only for lower-lying states. We will use an estimate based on a comparison of the results of  $B_{60}$  [19] and  $A_{60}$  [20] for states with  $l \geq 5$ , which suggests that the magnitude of  $B_{60}$  can be estimated to be about four times that of  $A_{60}$ . This will be used as the associated uncertainty. The three-photon diagrams lead to the  $C_{60}$  coefficient and have not been determined yet.

The calculation of the  $A_{60}$  coefficient has proved to be quite difficult. The problem is that this correction receives contributions from both high- and low-energy photons. For high-energy photons, perturbation theory in the Coulomb in-

teraction can be used, but for low-energy photons the Coulomb potential has to be treated in all orders. Therefore, the calculation is split into high- and low-energy parts. In the low-energy part, effective low-energy QED (NRQED) [21]

**Table 1.** Calculated values for the  $A_{60}$  coefficient.

$n$	$A_{60}$ for $l = n - 2, j = l - 1/2$	$A_{60}$ for $l = n - 1, j = l - 1/2$
9	7.018 373(5) $\times 10^{-5}$	3.860 349(5) $\times 10^{-5}$
10	3.655 111(5) $\times 10^{-5}$	2.158 923(5) $\times 10^{-5}$
11	2.008 438(5) $\times 10^{-5}$	1.259 580(5) $\times 10^{-5}$
12	1.019 187(5) $\times 10^{-5}$	0.759 620(5) $\times 10^{-5}$
13	0.679 575(5) $\times 10^{-5}$	0.469 973(5) $\times 10^{-5}$
14	0.410 825(50) $\times 10^{-5}$	0.296 641(5) $\times 10^{-5}$
15	0.252 108(5) $\times 10^{-5}$	0.189 309(5) $\times 10^{-5}$
16	0.155 786(5) $\times 10^{-5}$	0.121 749(5) $\times 10^{-5}$
$n$	$A_{60}$ for $l = n - 2, j = l + 1/2$	$A_{60}$ for $l = n - 1, j = l + 1/2$
9	28.939 225(5) $\times 10^{-5}$	14.918 400(5) $\times 10^{-5}$
10	16.589 245(5) $\times 10^{-5}$	9.141 150(5) $\times 10^{-5}$
11	10.111 871(5) $\times 10^{-5}$	5.882 197(5) $\times 10^{-5}$
12	6.331 080(5) $\times 10^{-5}$	3.940 256(5) $\times 10^{-5}$
13	4.318 998(5) $\times 10^{-5}$	2.729 475(5) $\times 10^{-5}$
14	2.979 937(5) $\times 10^{-5}$	1.945 279(5) $\times 10^{-5}$
15	2.116 050(5) $\times 10^{-5}$	2.420 631(5) $\times 10^{-5}$
16	1.540 181(5) $\times 10^{-5}$	1.059 674(5) $\times 10^{-5}$

**Note:** The numbers in parentheses are standard uncertainties in the last figure.

**Table 2.** Transition frequencies between the highest  $j$ -states with  $n = 14$  and  $n = 15$  in hydrogenlike helium and hydrogenlike neon.

Term	${}^4\text{He}^+$ $\nu$ (THz)	${}^{20}\text{Ne}^{9+}$ $\nu$ (THz)
$E_{\text{DM}}$	8.652 370 766 008(58)	216.335 625 574 6(14)
$E_{\text{RR}}$	0.000 000 000 000	0.000 000 0001
$E_{\text{QED}}$	-0.000 000 001 894	-0.000 001 184 1
Total	8.652 370 764 114(58)	216.335 624 390 7(14)

**Note:** The accuracy of the predicted frequencies is limited by the accuracy with which the Rydberg constant is currently known. A measurement of a transition frequency to an accuracy better than indicated in the table would lead to an improved determination of the Rydberg constant.

is used, which provides an all-order treatment of the potential. It also provides a separation into a radial and angular part of both the wave functions and the hydrogen Coulomb Green function. Both the high- and low-energy parts are matched together at the end of the calculation using an intermediate overlap parameter for which a number of reparameterization-invariant choices are available [22]. For Rydberg states, the angular algebra is quite complicated but could be handled with the use of computer algebra. In many calculations with the hydrogen Green function, a Sturmian decomposition is used for the radial part of the propagator. However for higher excited states, this leads to hypergeometric functions with high indices and thereby to an excessive number of terms. For example, the calculation of  $A_{60}$  for the 8D state using a Sturmian basis set leads to  $\sim 10^5$  terms in intermediate steps. As this trend continues for higher  $n$ , a calculation with this method for highly excited Rydberg states seems intractable.

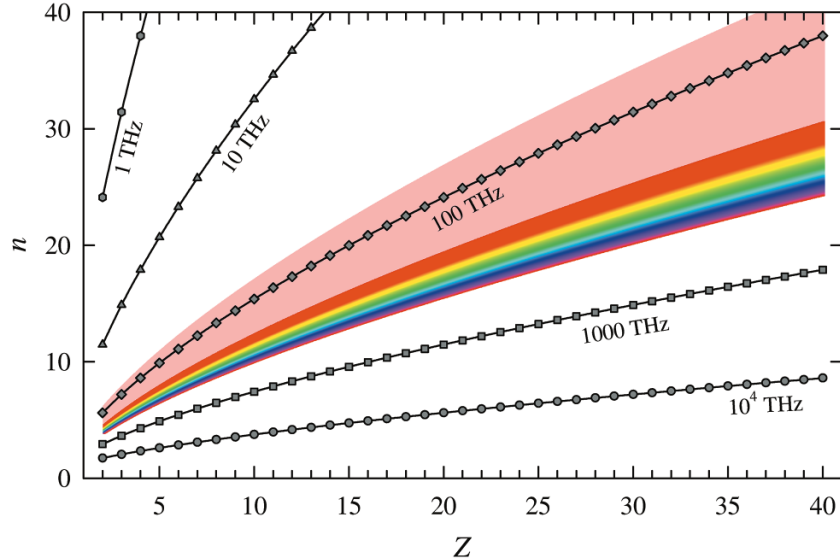
To solve this problem and to be able to calculate the  $A_{60}$  coefficient for Rydberg states, we employ a numerically determined, accurate basis set of wave functions for the Coulomb Green function. This also makes it possible to do the integration in the virtual photon energy analytically, making it easier to deal with the numerous poles along the virtual photon energy integration contour (the origin of the poles is due to spontaneous decays to lower levels). Strictly

**Table 3.** Sources and estimated relative standard uncertainties in the theoretical value of the transition frequency between the highest  $j$  states with  $n = 14$  and  $n = 15$  in hydrogenlike helium and hydrogenlike neon.

Source	$\text{He}^+$	$\text{Ne}^{9+}$
Rydberg constant	$6.6 \times 10^{-12}$	$6.6 \times 10^{-12}$
Fine-structure constant	$7.0 \times 10^{-16}$	$1.7 \times 10^{-14}$
Electron–nucleus mass ratio	$5.8 \times 10^{-14}$	$1.2 \times 10^{-14}$
$a_e$	$5.1 \times 10^{-20}$	$1.3 \times 10^{-18}$
Theory: $E_{\text{RR}}$ higher orders	$6.2 \times 10^{-17}$	$2.4 \times 10^{-14}$
Theory: $E_{\text{QED}} A_{81}$ coefficient	$1.7 \times 10^{-18}$	$1.6 \times 10^{-14}$
Theory: $E_{\text{QED}} B_{60}$ coefficient	$8.6 \times 10^{-18}$	$5.4 \times 10^{-15}$

speaking, the complete self-energy radiative correction to a reference level is a complex quantity,  $E_{\text{QED}} \rightarrow E_{\text{QED}} - i\Gamma/2$ . As the poles lead to an imaginary part, they contribute to the spontaneous radiative decay  $\Gamma$ . A principal-value prescription thus has to be used for the photon energy integrations, and it can be implemented in a very straightforward way using the analytic photon energy integration [22]. In a numerical integration, this would have to be implemented by subtracting the poles. Since the poles become more numerous for higher  $n$  states, the subtraction becomes more demanding.

**Fig. 2.** Graph showing values of  $Z$  and approximate  $n$  that give a specified value of the frequency for transitions between states with principal quantum number  $n$  and  $n - 1$  in a hydrogen-like ion with nuclear charge  $Z$ . Frequencies in the near infrared and visible range are indicated in color. Reprinted with permission from ref. 4. Copyright 2008 American Physical Society.



The problem with this approach is that a numerical radial integral over the complete radial basis set remains to be evaluated. Therefore, a numerical lattice method has been used [23]. By putting the atom in a box large enough to include the Rydberg state radial wave function and by discretising space, the Hamiltonian becomes a matrix, and therefore the complete basis set becomes finite and discrete. Thus, besides a finite and discrete bound state spectrum, this approach also yields a finite pseudo-spectrum of continuum states, which we represent in extended precision arithmetic. The results of a calculation of  $A_{60}$ , using this method for states with  $n = 9$  to  $n = 16$ , are given in Table 1.

As mentioned earlier, we concentrate on the real part of the energy shift, but the imaginary part can also have an influence on the frequencies measured in an experiment. The dominant decay for the highest  $l$  value of state  $n$ , which we consider here, is an electric dipole (E1) decay to the highest- $l$  value of the state  $n - 1$ . The nonrelativistic expression for this decay rate has been examined in [24] and also in [25] as the nonrelativistic limit of the imaginary part of the level shift. It is possible that this decay rate can introduce asymmetries into the line shape and the transition frequencies. Fortunately, these effects are small and of the order  $\alpha(Z\alpha)^2 \times E_{\text{QED}}$ , as has been shown by Low [26]. Should an analysis of these corrections become necessary, they can be calculated and determined for the systems chosen for the experiments, taking into account details of the experimental setup.

We have evaluated the final expressions for the energy shifts and for the transition frequencies in Table 2 using the values of the constants from CODATA 2006 [3]. We thereby make a theoretical prediction for the transition between the state with  $n = 14$ ,  $l = 13$ ,  $j = 27/2$  and the state with  $n = 15$ ,  $l = 14$ ,  $j = 29/2$  for hydrogenlike  $\text{He}^+$  and  $\text{Ne}^{9+}$ . The neon nuclear mass  $m(^{20}\text{Ne}^{9+})$  is taken from a measurement [27], corrected for the mass of the electrons and their binding energies. The standard uncertainty of each contribution is given in brackets if it is not negligible.

In Table 3 we list all major sources of uncertainty and give estimates of their size. Again, we see that the Rydberg constant is the largest source of uncertainty, confirming that an experimental determination of a transition frequency to better accuracy could enhance the level of accuracy of this fundamental constant. This is in contrast to the 1S–2S transition, where the relative uncertainty from the two-photon  $B_{60}$  term is already of relative order of  $10^{-12}$  due to a disagreement between different calculations and due to the (possibly large) numerical values of the unknown,  $B_{72}$ ,  $B_{71}$ , and  $B_{70}$  terms (which are nonvanishing for S states). These give the higher-order two-loop binding corrections.

### 3. Conclusion

By using Rydberg states of hydrogenlike ions with a medium nuclear charge number (e.g., neon with  $Z = 10$ ), a number of problems associated with either higher-order binding corrections to QED interactions or the nuclear size effect in Lamb shift predictions can essentially be avoided. The higher-order QED binding corrections for Rydberg states are smaller by a factor of about  $10^6$  compared with S states, which provides significant advantages from a theoretical point of view. A suitable combination of  $n$  and  $Z$  has to be found so that the transition frequency lies in the optical or near-infrared regime. The range of such values is shown in Fig. 2. Low- $Z$  ions seem to be the most favorable systems for a frequency comb measurement, while in heavier ions with larger  $Z$  some perturbations are smaller. So using many different combinations of  $n$  and  $Z$  may be useful for experimental checks and optimization. An approach based on highly-excited states might lead to a new determination of the Rydberg constant, based on a combination of theory and experiment. With the new values for the  $A_{60}$  coefficients presented here in Table 1, the diversity of transitions available for the project is enlarged in comparison to the previous proposal [4].

## Acknowledgments

BJW acknowledges support from the Deutsche Forschungsgemeinschaft. UDJ acknowledges support from the National Science Foundation (Grant PHY-8555454) and from the Missouri Research Board.

## References

1. T.W. Hänsch. *Rev. Mod. Phys.* **78**, 1297 (2006). doi:10.1103/RevModPhys.78.1297.
2. T.W. Hänsch, J. Alnis, P. Fendel, M. Fischer, C. Gohle, M. Herrmann, R. Holzwarth, N. Kolachevsky, Th. Udem, and M. Zimmermann. *Philos. Trans. R. Soc. London, Ser. A*, **363**, 2155 (2005). doi:10.1098/rsta.2005.1639.
3. P.J. Mohr, B.N. Taylor, and D.B. Newell. *Rev. Mod. Phys.* **80**, 633 (2008). doi:10.1103/RevModPhys.80.633.
4. U.D. Jentschura, P.J. Mohr, J.N. Tan, and B.J. Wundt. *Phys. Rev. Lett.* **100**, 160404 (2008). doi:10.1103/PhysRevLett.100.160404.
5. J.C. De Vries. Ph.D. thesis. MIT, Boston, Mass., USA. 2001.
6. M.I. Eides, H. Grotch, and V.A. Shelyuto. *Phys. Rep.* **342**, 63 (2001). doi:10.1016/S0370-1573(00)00077-6.
7. G.W. Erickson. *J. Phys. Chem.* **6**, 833 (1977).
8. K. Pachucki. *J. Phys. B*, **31**, 5123 (1998). doi:10.1088/0953-4075/31/23/010.
9. K. Pachucki and H. Grotch. *Phys. Rev. A*, **51**, 1854 (1995). doi:10.1103/PhysRevA.51.1854.
10. M.I. Eides and H. Grotch. *Phys. Rev. A*, **55**, 3351 (1997). doi:10.1103/PhysRevA.55.3351.
11. E.A. Golosov, A.S. Elkhovskiy, A.I. Milstein, and I.B. Khriplovich. *Zh. Eksp. Teor. Fiz.* **107**, 393 [*JETP* **80**, 208 (1995)].
12. A.S. Elkhosky. *Zh. Eksp. Teor. Fiz.* **110**, 431 [*JETP* **83**, 230 (1996)].
13. U.D. Jentschura and K. Pachucki. *Phys. Rev. A*, **54**, 1853 (1996). doi:10.1103/PhysRevA.54.1853.
14. K. Melnikov and A. Yelkhosky. *Phys. Lett.* **458B**, 143 (1999).
15. K. Pachucki and S.G. Karshenboim. *Phys. Rev. A*, **60**, 2792 (1999). doi:10.1103/PhysRevA.60.2792.
16. D. Hanneke, S. Fogwell, and G. Gabrielse. *Phys. Rev. Lett.* **100**, 120801 (2008). doi:10.1103/PhysRevLett.100.120801.
17. E.H. Wichmann and N.M. Kroll. *Phys. Rev.* **101**, 843 (1956). doi:10.1103/PhysRev.101.843.
18. U.D. Jentschura, A. Czarnecki, and K. Pachucki. *Phys. Rev. A*, **72**, 062102 (2005). doi:10.1103/PhysRevA.72.062102.
19. U.D. Jentschura. *Phys. Rev. A*, **74**, 062517 (2006). doi:10.1103/PhysRevA.74.062517.
20. E.-O. Le Bigot, U.D. Jentschura, P.J. Mohr, P. Indelicato, and G. Soff. *Phys. Rev. A*, **68**, 042101 (2003). doi:10.1103/PhysRevA.68.042101.
21. W. Caswell and G. Lepage. *Phys. Lett. B*, **167**, 437 (1986). doi:10.1016/0370-2693(86)91297-9.
22. B.J. Wundt and U.D. Jentschura. *Phys. Lett. B*, **659**, 571 (2008). doi:10.1016/j.physletb.2007.11.062.
23. S. Salomonson and P. Öster. *Phys. Rev. A*, **40**, 5559 (1989). doi:10.1103/PhysRevA.40.5559.
24. H.A. Bethe and E.E. Salpeter. *Quantum mechanics of one- and two-electron atoms*. Academic, New York, USA. 1957.
25. U.D. Jentschura, E.-O. Le Bigot, J. Evers, P.J. Mohr, and C.H. Keitel. *J. Phys. B*, **38**, S97 (2005). doi:10.1088/0953-4075/38/2/008.
26. F. Low. *Phys. Rev.* **88**, 53 (1952). doi:10.1103/PhysRev.88.53.
27. G. Audi, A.H. Wapstra, and C. Thibault. *Nucl. Phys. A*, **729**, 337 (2003). doi:10.1016/j.nuclphysa.2003.11.003.